J. Fluid Mech. (1987), *vol.* 185, *pp.* 523–545
Printed in Great Britain

The runup of solitary waves

By COSTAS EMMANUEL SYNOLAKIS
School of Engineering, University of Southern California, Los Angeles, California 90089-0242, USA

(Received 22 August 1986 and in revised form 9 May 1987)

This is a study of the runup of solitary waves on plane beaches. An approximate theory is presented for non-breaking waves and an asymptotic result is derived for the maximum runup of solitary waves. A series of laboratory experiments is described to support the theory. It is shown that the linear theory predicts the maximum runup satisfactorily, and that the nonlinear theory describes the climb of solitary waves equally well. Different runup regimes are found to exist for the runup of breaking and non-breaking waves. A breaking criterion is derived for determining whether a solitary wave will break as it climbs up a sloping beach, and a different criterion is shown to apply for determining whether a wave will break during rundown. These results are used to explain some of the existing empirical runup relationships.

1. Introduction

The problem of determining the runup of solitary waves on plane beaches usually arises in the study of the coastal effects of tsunamis. Tsunamis are long water waves of small steepness generated by impulsive geophysical events on the ocean floor or at the coastline. Solitary waves are believed to model some important aspects of the coastal effects of tsunamis well.

The process of long-wave generation and propagation is now well understood. The process of long-wave runup and reflection is not. Although there is consensus that a suitable physical model for this process is the formalism of a long wave propagating over constant depth and encountering a sloping beach, there is little agreement on the appropriate analytical formulation. The analytical studies of this problem can be classified in two general groups depending on the approximation of the equations of motion that was used in each study to determine the runup.

One group has studied variants of the Boussinesq equations. The state-of-the-art numerical solutions of these equations for solitary-wave runup are those of Pedersen & Gjevik (1983) and Zelt (1986) who solved the equations in Lagrangian coordinates, and of Kim, Liu & Ligett (1983) who used boundary-integral methods.

The other group has used the shallow-water-wave equations. These two nonlinear equations result directly from the Boussinesq equations, if the effects of dispersion and vertical accelerations are neglected. A comprehensive review of various regular, weak and apparent solutions of these equations may be found in Meyer (1986). The classic solution of their linear form was given by Lewy (1946) for the problem of periodic waves climbing up a sloping beach. Carrier & Greenspan (1958) derived a nonlinear transformation to reduce the two equations to a single linear equation and they solved several initial-value problems. Keller & Keller (1964) solved the linear problem of a periodic wave propagating first over constant depth and then up a

sloping beach. Carrier (1966) used the Carrier & Greenspan transformation to calculate in closed form the runup of a wave generated by a bottom displacement and propagating over relatively arbitrary bathymetry. The state-of-the-art numerical solution of the nonlinear equations was achieved with the work of Hibberd & Peregrine (1979); they were able to calculate the runup of a uniform bore on a plane beach.

Despite the quality of the analytical work, fundamental unresolved questions about the runup of long waves still exist. The empirical relationship between the normalized runup and the normalized wave height that has been established in the series of laboratory investigations of Hall & Watts (1953), Camfield & Street (1969), and Kishi & Saeki (1966) remains unexplained analytically. The results of the available numerical solutions have not been compared with detailed amplitude-evolution data from the laboratory, and, as a consequence, there is little conclusive information about the relative importance of dispersion and nonlinearity during runup. There is no realization of the differences in the runup behaviour of breaking and non-breaking waves, and this has led to numerical results for non-breaking waves to be compared with laboratory data for breaking waves. Compared with recent advances in periodic-wave runup (Guza & Thornton 1982; Holman 1986), the understanding of solitary-wave runup has been fragmented and incomplete.

In the present study an exact solution to an approximate theory will be presented for determining the runup and the amplitude evolution of long waves on plane beaches. A series of experiments will also be described and the resolution of some of these questions will be attempted.

2. Basic equations and solutions

Consider a topography consisting of a plane sloping beach of angle β, as shown in figure 1. The origin of the coordinate system is at the initial position of the shoreline and $\tilde{x}$ increases seaward. Dimensionless variables are introduced as follows:

$$\tilde{x} = xd, \quad \tilde{h}_0 = h_0 d, \quad \tilde{\eta} = \eta d, \quad \tilde{u} = u(gd)^{\frac{1}{2}}, \quad \tilde{t} = t(d/g)^{\frac{1}{2}}.$$

η is the amplitude, u is the depth-averaged velocity, and h_0 is the undisturbed water depth. The topography is described by

$$h_0(x) = x \tan\beta \quad \text{when } x \leqslant \cot\beta \tag{2.1a}$$

and

$$h_0(x) = 1 \quad \text{when } x > \cot\beta. \tag{2.1b}$$

Consider a propagation problem described by the shallow-water-wave equations

$$h_t + (hu)_x = 0 \tag{2.2a}$$

and

$$u_t + uu_x + \eta_x = 0, \tag{2.2b}$$

where $h(x,t) = h_0(x) + \eta(x,t)$.

2.1. *Linear theory*

The system of equations (2.2) can be linearized by retaining the first-order terms only. The following equation results:

$$\eta_{tt} - (\eta_x h_0)_x = 0. \tag{2.3}$$

The solution for constant depth is

$$\eta(x,t) = A_i \, e^{-ik(x+ct)} + A_r \, e^{ik(x-ct)} \quad \text{when } h_0(x) = 1, \tag{2.4a}$$

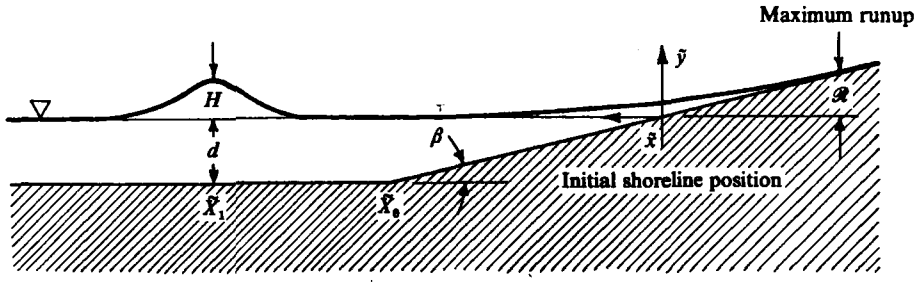

FIGURE 1. A definition sketch for a solitary wave climbing up a sloping beach. All variables except β are dimensional.

and the solution for variable depth and finite at the shoreline is

$$\eta(x,t) = B(k,\beta)J_0(2k(x\cot\beta)^{\frac{1}{2}})\,\mathrm{e}^{-\mathrm{i}kct} \quad \text{when } h_0(x) = x\tan\beta. \tag{2.4b}$$

A_1 is the amplitude of the incident wave, A_r that of the reflected wave, B is the amplification factor, k is the wavenumber and $c = 1$. Keller & Keller (1964) presented another steady-state solution for the combined topography defined by (2.1). They matched the outer solution (2.4*a*) and its x-slope to the inner solution (2.4*b*) and its x-slope, at $x = X_0 = \cot\beta$, the toe of the beach, and they derived the following values for the reflected-wave amplitude and the amplification factor for an incident wave of the form $\eta(x,t) = A_1\,\mathrm{e}^{-\mathrm{i}(x+ct)}$:

$$A_r(k,\beta,A_1) = A_1\exp\left[-2\mathrm{i}k\cot\beta + 2\arctan\frac{J_1(2k\cot\beta)}{J_0(2k\cot\beta)}\right] \tag{2.5a}$$

and

$$B(k,\beta,A_1) = \frac{2\exp[-\mathrm{i}k\cot\beta]A_1}{J_0(2k\cot\beta) - \mathrm{i}J_1(2k\cot\beta)}. \tag{2.5b}$$

2.2. *Exact solutions of the linear theory*

This formalism will now be used to study the behaviour of more general waveforms approaching the sloping beach. Since the governing equation (2.3) is linear and homogeneous, then, as Stoker (1947) pointed out, the standing-wave solution (2.4) can be used to obtain travelling-wave solutions by linear superposition. When a boundary condition is specified, the solution follows directly from the Fourier transform of the equation. For example, when the incident wave is of the form

$$\eta(X_0,t) = \int_{-\infty}^{\infty}\Phi(k)\,\mathrm{e}^{-\mathrm{i}kct}\,\mathrm{d}k,$$

then the transmitted wave to the beach is given by

$$\eta(x,t) = 2\int_{-\infty}^{\infty}\Phi(k)\frac{J_0(2k(xX_0)^{\frac{1}{2}})\,\mathrm{e}^{-\mathrm{i}k(X_0+ct)}}{J_0(2kX_0) - \mathrm{i}J_1(2kX_0)}\mathrm{d}k. \tag{2.6}$$

This solution is only valid when $x \geqslant 0$; when $x < 0$, (2.3) does not reduce to Bessel's equation. To obtain details of the motion in this case, one must solve the nonlinear set (2.2).

When initial values are available, it is necessary to use a different method. The standard practice is to use Hankel transform techniques; the substitution $\zeta = x^{\frac{1}{2}}$ transforms (2.3) into the equation: $\eta_{\zeta\zeta} + (1/\zeta)\eta_\zeta = 4\cot\beta\eta_{tt}$, and the solution follows

directly as a Hankel transform integral (Carrier 1966; Tuck & Hwang 1972). Alternatively, one may use the expansion

$$\eta(\zeta, t) = \sum_{n=1}^{\infty} c_n(t) J_0(j_n \zeta),$$

where j_n is the nth zero of J_0. The coefficients of the Fourier–Bessel series can be found directly from the series expansion by using the orthogonality properties of the Bessel functions:

$$c_n(t) = \frac{2}{J_1(j_n)^2} \int_0^1 s J_0(j_n s)\, \eta(s, t)\, \mathrm{d}s$$

s is the integration variable. $c_n(t)$ can then be determined explicitly from

$$\frac{\mathrm{d}^2 c_n}{\mathrm{d}t^2} = -\tfrac{1}{4} j_n^2 c_n$$

and the appropriate initial conditions. A similar solution is presented in Carrier, Krook & Pearson (1966) for an equation that describes the motion of a hanging chain.

2.3. *Nonlinear theory*

To solve the nonlinear set (2.2) for the sloping-beach case, $h_0(x) = x \tan\beta$, Carrier & Greenspan (1958) proceeded to consider the independent variables x, t as functions of the Riemann invariants of the hyperbolic system and, after some effort, they were able to deduce the following hodograph transformation, (referred to as the C&G transformation for short):

$$u = \frac{\psi\sigma}{\sigma}, \tag{2.7a}$$

$$x = \cot\beta(\tfrac{1}{16}(\sigma^2 - \tfrac{1}{4}\psi_\lambda + \tfrac{1}{2}u^2)), \tag{2.7b}$$

$$t = \cot\beta\left(\frac{\psi_\sigma}{\sigma} - \tfrac{1}{2}\lambda\right), \tag{2.7c}$$

and

$$\eta = \tfrac{1}{4}\psi_\lambda - \tfrac{1}{2}u^2, \tag{2.7d}$$

which reduces the set (2.2) to a single linear equation,

$$(\sigma\psi_\sigma)_\sigma = \sigma\psi_{\lambda\lambda}. \tag{2.8}$$

The transformation is such that in the hodograph plane, i.e. the (σ,λ)-space, the shoreline is always at $\sigma = 0$; this can be deduced easily by setting $\sigma = 0$ in (2.7b) and by observing that then $x = -\eta\cot\beta$, which is an equality only valid at the shoreline tip.

2.4. *Exact solutions of the nonlinear theory*

Equation (2.8) can be solved with standard methods. When a boundary condition is specified, then the method of choice is the Fourier transform technique. Defining the Fourier transform of $\psi(\sigma, \lambda)$ as

$$\Psi(\sigma, \tilde{k}) = \int_{-\infty}^{\infty} \psi(\sigma, \lambda)\, \mathrm{e}^{-\mathrm{i}\lambda\tilde{k}}\, \mathrm{d}\lambda,$$

and, if $\Psi(\sigma_0, \tilde{k}) = F(\tilde{k})$, then the bounded solution at $\sigma = 0$ and $\sigma = \infty$ takes the form

$$\psi(\sigma, \lambda) = \frac{1}{2\pi} \int_{-\infty}^{\infty} F(\tilde{k}) \frac{J_0(\tilde{k}\sigma)}{J_0(\tilde{k}\sigma_0)}\, \mathrm{e}^{\mathrm{i}\tilde{k}\lambda}\, \mathrm{d}\tilde{k}. \tag{2.9}$$

If an initial condition is available instead, then one may use Hankel transform methods (Carrier 1966), or proceed as suggested in §2.2.

To complete the solution of (2.8) an appropriate initial or boundary condition has to be specified explicitly. Carrier & Greenspan (1958) presented a general solution to an initial-value problem where the initial velocity $u(x, t_0)$ is zero. Spielvogel (1974) used this solution to derive the evolution of a wave during rundown, assuming an initially exponentially shaped runup profile. Carrier & Greenspan also presented certain solutions with $u(x, t_0) \neq 0$, but for very specific initial conditions.. Tuck & Hwang (1972) also solved the initial-value problem.

In general, it is difficult to specify initial or boundary data on the sloping beach without making restrictive assumptions about the solution; a boundary condition requires specification of the solution at $(x_0, \forall t)$, and an initial-condition specification at $(t_0, \forall x)$, but in practice the solution is only known at $(x_0 \geqslant \cot\beta,\ t < t_0)$, where t_0 is the time when the wave reaches the x-location x_0. Even when boundary or initial conditions are available in the (x, t)-space, the process of deriving the equivalent conditions in the (σ, λ)-space is not trivial.

These difficulties have restricted the use of the Carrier & Greenspan formalism to problems that can be reduced directly to those solved by Carrier & Greenspan. This is unfortunate because some of the problems described can be circumvented. Carrier (1966) demonstrated how to specify a boundary condition when reflection from the beach is negligible. Another method will be presented here to specify a boundary condition including reflection.

2.5. *Approximate solution of the nonlinear theory*

Carrier (1966) pointed out that far from the shoreline nonlinear effects are small. The transformation equations can then be simplified by neglecting $O(u^2)$ terms. To the same order, $\psi_\lambda \ll \frac{1}{16}\sigma^2$ and $\psi_\sigma/\sigma \ll \frac{1}{2}\lambda$. Using these approximations, the set of equations (2.7) becomes

$$u = \frac{\psi_\sigma}{\sigma}, \quad \eta = \tfrac{1}{4}\psi_\lambda, \quad x = \tfrac{1}{16}\sigma^2 \cot\beta, \quad t = -\tfrac{1}{2}\lambda \cot\beta. \tag{2.10}$$

These equations are uncoupled and allow direct transition from the (σ, λ) to the (x, t)-space.

One method for specifying a boundary condition in the physical space is to use the solution of the equivalent linear problem, as given by (2.8). This is formally correct to the same order of approximation as (2.10). The obvious choice for the specification is the seaward boundary; it is desirable to use the linearized form of the equation of motion at the furthest possible location from the initial position of the shoreline where the Carrier & Greenspan formalism is valid. This is the point $x = X_0 = \cot\beta$ and it corresponds to the point $\sigma = \sigma_0 = 4$ in the (σ, λ)-space. Then (2.10) implies that $\eta(X_0, t) = \frac{1}{4}\psi_\lambda(4, \lambda)$. The boundary condition $F(\tilde{k})$ in the (σ, λ)-space is then determined from (2.29) by repeated application of the Fourier integral theorem. Assuming that $\psi(\sigma_0, \lambda) \to 0$ as $\lambda \to \pm\infty$, then the solution of (2.8) follows:

$$\psi(\sigma, \lambda) = -\frac{16\mathrm{i}}{X_0} \int_{-\infty}^{\infty} \frac{\Phi(\kappa)}{\kappa} \frac{J_0(\frac{1}{2}\sigma\kappa X_0) \exp[-\mathrm{i}\kappa X_0(1-\frac{1}{2}\lambda)]}{J_0(2\kappa X_0) - \mathrm{i}J_1(2\kappa X_0)} \mathrm{d}\kappa; \tag{2.11}$$

the substitution $\kappa = (2/X_0)\tilde{k}$ was used to simplify the expression.

2.6. *Runup invariance in the linear and nonlinear theory*

It is interesting to compare the predictions of the linear and nonlinear theory for the maximum runup and minimum rundown. It will be proved that they are identical. The maximum runup according to the linear theory is the maximum value attained by the wave amplitude at the initial position of the shoreline $x = 0$, or

$$\eta(0,t) = 2\int_{-\infty}^{\infty} \frac{\Phi(k)\exp[-ik(X_0+ct)]}{J_0(2kX_0)-iJ_1(2kX_0)}\mathrm{d}k. \tag{2.12}$$

In the nonlinear theory the maximum runup is given by the maximum value of the amplitude at the shoreline $\eta(x_s,\lambda)$. (x_s is the x-coordinate of the shoreline and it corresponds to $\sigma = 0$.) To determine $\eta(x_s,\lambda)$ one can use (2.7d) to obtain

$$\eta(x_s,t) = \tfrac{1}{4}\psi_\lambda - \tfrac{1}{2}u_s^2 = 2\int_{-\infty}^{\infty} \frac{\Phi(\kappa)\exp[-i\kappa X_0(1-\frac{1}{2}\lambda)]}{J_0(2\kappa X_0)-iJ_1(2\kappa X_0)}\mathrm{d}\kappa - \tfrac{1}{2}u_s^2; \tag{2.13}$$

$u_s = \mathrm{d}x_s/\mathrm{d}t$ is the velocity of the shoreline tip.

At the point of maximum runup the velocity of the shoreline tip becomes zero. Setting $u_s = 0$ and $\sigma = 0$ in the transformation equations (2.7) reduces them to

$$u = 0, \quad \eta = \tfrac{1}{4}\psi_\lambda, \quad x = -\eta\cot\beta, \quad t = -\tfrac{1}{2}\lambda\cot\beta. \tag{2.14}$$

Substitution of these values in (2.13) reduces it to (2.12), proving that the maximum runup predicted by the linear theory is identical with the maximum runup predicted by the nonlinear theory. The same argument applies at the point of minimum rundown where the shoreline tip also attains zero velocity. This invariance was first noted by Carrier (1971) who observed that the maximum runup is given correctly by a linear theory (presumably (2.8)) as the maximum value of $\eta = \frac{1}{4}\psi_\lambda$. However, Carrier did not present an actual comparison between linear and nonlinear theory for polychromatic waveforms, and this result has been largely unrecognized. It is unexpected, because, as will be shown later, the amplitude-evolution data derived using the linear and the nonlinear theory differ most at the initial shoreline (see, for example, figure 5).

3. The solitary-wave solution

The results of the previous section will now be applied to derive a result for the maximum runup of a solitary wave climbing up a sloping beach. A solitary wave centred at $x = X_1$ at $t = 0$ has the following surface profile:

$$\eta(x,0) = \frac{H}{d}\operatorname{sech}^2\gamma(x-X_1), \tag{3.1}$$

where $\gamma = (3H/4d)^{\frac{1}{2}}$. The function $\Phi(k)$ associated with this profile is derived in Synolakis (1986) and it is given by

$$\Phi(k) = \tfrac{2}{3}k\operatorname{cosech}(\alpha k)\,\mathrm{e}^{ikX_1}, \tag{3.2}$$

where $\alpha = \pi/2\gamma$. Substituting this form into (2.12) and defining as $\tilde{R}(t)$ the dimensional surface elevation at the initial position of the shoreline, then the following relationship results:

$$\frac{\tilde{R}(t)}{d} = \frac{4}{3}\int_{-\infty}^{\infty} k\operatorname{cosech}(\alpha k)\frac{\exp[ik(X_1-X_0-ct)]}{J_0(2kX_0)-iJ_1(2kX_0)}\mathrm{d}k. \tag{3.3}$$

This integral can be calculated with standard methods of applied mathematics; its convergence and evaluation is discussed in the Appendix. The integration result is

$$\frac{\tilde{R}(t)}{d} = 8\frac{H}{d}\sum_{n=1}^{\infty}\frac{(-1)^{n+1}n\exp\left[-2\gamma(X_1-X_0-ct)\,n\right]}{I_0(4\gamma X_0 n)+I_1(4\gamma X_0 n)}. \tag{3.4}$$

The series can be simplified further by using the asymptotic form for large arguments of the modified Bessel functions. When $4X_0\gamma \gg 1$, then

$$\frac{\tilde{R}(t)}{d} = 8(\pi X_0)^{\frac{1}{4}}\frac{H}{d}\left(3\frac{H}{d}\right)^{\frac{1}{4}}\sum_{n=1}^{\infty}(-1)^{n+1}n^{\frac{3}{4}}\exp\left[-2\gamma(X_1+X_0-ct)\,n\right]. \tag{3.5}$$

This form of the solution is particularly helpful for calculating the maximum runup. The series in (3.5) is of the form

$$\sum_{n=1}^{\infty}(-1)^{n+1}n^{\frac{3}{4}}\chi^n;$$

its maximum value occurs at $\chi = 0.481 = \mathrm{e}^{-0.732}$. This value defines the time $t_{\max}$ when the wave reaches its maximum runup as

$$t_{\max} = \frac{1}{c}\left(X_1+X_0-\frac{0.366}{\gamma}\right). \tag{3.6}$$

The value of the series (3.5) at $t_{\max}$ is $s_{\max}$ and $s_{\max} = 0.15173$. Defining as $\mathscr{R}$ the maximum value of $\tilde{R}(t)$ and evaluating the term $8(\pi\sqrt{3})^{\frac{1}{4}}s_{\max}$ then the following expression results for the maximum runup:

$$\frac{\mathscr{R}}{d} = 2.831\,(\cot\beta)^{\frac{1}{2}}\left(\frac{H}{d}\right)^{\frac{5}{4}}. \tag{3.7}$$

This equation will be henceforth referred to as *the runup law*. It is formally correct when $(H/d)^{\frac{1}{2}} \gg 0.288\tan\beta$ – the assumption implied when using the asymptotic form of the Bessel functions – and when the series converges as discussed in the Appendix. The same result can also be derived by calculating ψ_λ from the nonlinear-theory solution (2.11) and then using the appropriate equations (2.14) for the shoreline motion.

To derive surface profiles in the entire flow domain it is necessary to use the nonlinear theory and solve the transformation equations (2.7). The solution is given by

$$u = \frac{\psi_\sigma}{\sigma}$$

$$= \frac{16\mathrm{i}}{3}\int_{-\infty}^{\infty}\kappa\,\mathrm{cosech}\,(\alpha\kappa)\frac{J_1(\frac{1}{2}\sigma\kappa X_0)\exp\left[\mathrm{i}\kappa(X_1-X_0+\frac{1}{2}\lambda X_0)\right]}{\sigma(J_0(2\kappa X_0)-(\mathrm{i}J_1(2\kappa X_0))}\mathrm{d}\kappa, \tag{3.8a}$$

$$\eta = \tfrac{1}{4}\psi_\lambda - \tfrac{1}{2}u^2$$

$$= \frac{4}{3}\int_{-\infty}^{\infty}\kappa\,\mathrm{cosech}\,(\alpha\kappa)\frac{J_0(\frac{1}{2}\sigma\kappa X_0)\exp\left[\mathrm{i}\kappa(X_1-X_0+\frac{1}{2}\lambda X_0)\right]}{J_0(2\kappa X_0)-\mathrm{i}J_1(2\kappa X_0)}\mathrm{d}\kappa - \tfrac{1}{2}u^2, \tag{3.8b}$$

$$x = \cot\beta\left(\frac{\sigma^2}{16}-\eta\right), \tag{3.8c}$$

and

$$t = \cot\beta\left(\frac{\psi_\sigma}{\sigma}-\tfrac{1}{2}\lambda\right). \tag{3.8d}$$

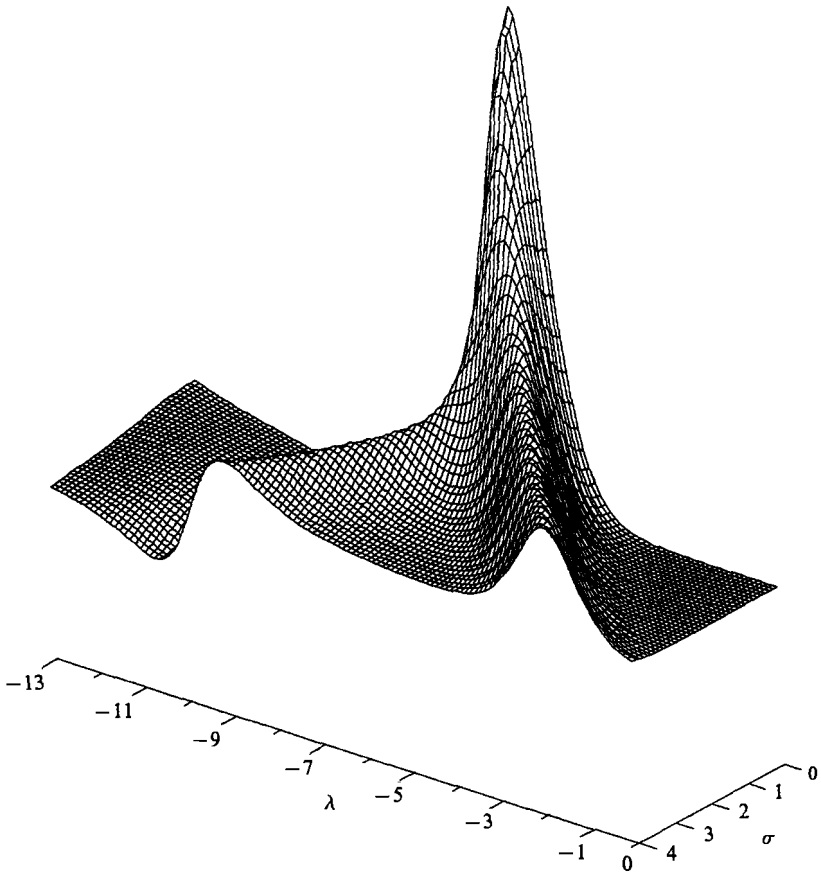

FIGURE 2. The function $\psi_\lambda(\sigma, \lambda)$ defined by (3.9) for a solitary wave with $H/d = 0.019$ up a beach with $\cot\beta = 19.85$.

The integrals in these equations can be evaluated directly for given (σ, λ) using the formalism of the Appendix. The function ψ_λ is shown in figure 2 as a function of (σ, λ) for the case when $H/d = 0.019$, $X_0 = 19.85$ and $X_1 = 37.35$. The amplitude evolution predicted by (3.8*b*) is discussed in §5.2, where it is compared with laboratory data obtained with the methods discussed next.

4. Experimental equipment

A series of laboratory experiments was conducted to investigate the validity of the results derived in the previous sections. The experiments were performed in the 40 m wave-tank facility of the W. M. Keck Laboratories of the California Institute of Technology. The facility consists of a wave tank, a wave generation system and a wave measuring system. The experimental equipment is detailed in Hammack (1972), Goring (1978) and Synolakis (1986).

The wave tank has glass sidewalls and dimensions 37.73 m × 0.61 m × 0.39 m. At one end of the tank and at a distance of 14.68 m from the wave generator a sloping beach was constructed; it consisted of a ramp made out of anodized aluminium panels with a hydrodynamically smooth surface. The ramp was supported with a wooden truss which was surveyed periodically to ensure that it conformed to the

initial 1:19.85 slope. For brevity, the ramp will be referred to as the laboratory beach.

The wave generation system consists of a piston attached to vertical wave plate which moves horizontally and displaces the adjacent fluid thereby generating waves. The piston is driven by a doubly actuated hydraulic cylinder controlled by a servo-valve which can be programmed to produce any desired piston motion. The system was interfaced with a PDP11/23 microprocessor which provided the required piston trajectory. The generation algorithm developed by Goring (1978) and generalized by Synolakis (1986) was used to compute the trajectory. The laboratory equipment produced near-perfect solitary waves; near-perfect refers to waves that conform to the Boussinesq profile (3.1) and have a tail that does not exceed 2% of the wave height H.

To measure wave heights in the constant-depth region parallel-wire resistance-type wave gauges were used. The gauges are constructed of steel wire of diameter 0.025 cm and can be calibrated to measure wave heights as small as 0.1 cm. They are driven by HP8701 Carrier preamplifiers. However, these gauges cannot be used close to the shoreline; the small local depths do not permit *in situ* calibration, and the gauges cannot be calibrated offshore and moved back, because of strong boundary effects over the beach. (One notable success in measuring wave heights on the dry bed with conventional gauges has been in the work of Battjes & Roos 1974.)

A new type of transducer was developed for this study, referred to as the runup gauge. It consists of an array of capacitance wave probes mounted on a π-shape aluminium frame. The distance between the probes is variable. The effective measuring length of each transducer and its distance from the tank bottom surface can be adjusted by sliding the probe inside its support bracket. In all applications in this study the transducers were equispaced and of the same length, and the tip of each probe was 0.1 cm from the tank bottom surface. Each probe is made of steel wire of 0.076 cm diameter it is fitted in a glass capillary tube which acts as the dielectric of the capacitor. The electronics design allows all probes to operate at the same frequency without any cross-talk between them. To calibrate, the runup gauge was moved in a programmed fashion down the ramp and changes in depth and voltage were recorded; there was no influence in the calibration data from wall effects because the probes maintained the same distance from the sloping bottom at every calibration step. This operation provided flexibility for deployment at different locations, and it allowed for wave-height measurements on the dry bed.

The runup gauge was tested dynamically by comparing its output to that of a conventional parallel-wire resistance-type gauge in the region of the tank where both types of transducers could be employed ($x > 10$); the comparison produced identical results. To test its performance in measuring wave runup on a dry bed, the runup gauge was deployed at a distance of -0.5 depths from the initial shoreline, with an interprobe spacing of 3.31 cm, while a movie camera was simultaneously recording the climb of a wave. The runup-gauge results were consistently within 3% of the movie data, a difference that may be attributed to errors inherent in the processing of cinematographic data.

The output of all transducers was recorded digitally through the Ad11K interface of a PDP11/23 microprocessor. Typically, sixteen channels of data were recorded at an intersample rate of either 0.004 or 0.008 s. Analysis and display of the data were performed in real time.

5. Experimental results

In this section the experimental results are compared to the theory advanced in §2. Maximum runup data from this and other investigations are presented in §5.1. In §5.2, measured surface profiles are compared with the linear and the nonlinear theory. Additional laboratory data are presented in §6, where the validity of the theory is discussed.

5.1. *Maximum runup*

The maximum-runup data for breaking and non-breaking solitary waves on the laboratory beach are presented in figure 3 and they are also listed in table 1. The parameter H/d represents the maximum normalized wave height measured at a distance L from to toe of the beach, where L is one measure of the horizontal extent of the wave, and

$$L = \frac{1}{\gamma}\operatorname{arccosh}\left[\left(\frac{1}{0.05}\right)^{\frac{1}{2}}\right], \tag{5.1}$$

where $\gamma = (3H/4k)^{\frac{1}{2}}$. Thus, heights of longer waves were measured further from the beach than of shorter waves, assuring that all waves propagated through the same relative distance L between the measurement location and the toe of the beach. The parameter $\mathscr{R}/d$ is the maximum excursion of the shoreline at the instant of maximum runup. Possibly owing to sidewall effects, the shoreline assumed a parabolic shape, in plan view. The runup distances defined with the minimum, average and maximum position of the shoreline at the instant of maximum exhibit similar dependence on the height-to-depth ratio. For example, for the breaking-wave data the dependence of maximum runup based on the maximum position of the shoreline is

$$\frac{\mathscr{R}}{d} = 1.109\left(\frac{H}{d}\right)^{0.582},$$

and based on the average position of the shoreline it takes form

$$\frac{\mathscr{R}}{d} = 0.918\left(\frac{H}{d}\right)^{0.606}.$$

The two-dimensional character of the shoreline was repeatable and it was more prevalent in the breaking-wave data.

Figure 3 includes data from experiments at different flow depths d, where 6.25 cm $< d <$ 38.32 cm. Pedersen & Gjevik (1983) reported experiments where the empirical runup relationships were influenced by the depth. However, in the present investigation and in the Hall & Watts (1953) study, a wave of a particular height-to-depth ratio realized similar normalized runup distances at different depths, as it would be expected from dimensional considerations.

Figure 3 shows distinct runup regimes for breaking and non-breaking waves. Breaking on the laboratory beach occurs first during the backwash when $H/d >$ 0.044; breaking during runup occurs when $H/d > 0.055$. The asymptotic result (3.7) is valid for waves that do not break during runup, suggesting that it is appropriate to use the qualifier non-breaking for waves that do not break during runup but may not break during rundown. This definition was used in preparing figure 3. The asymptotic result appears to be describing the *non-breaking*-wave data quite well.

The existence of the two different runup regimes has never been observed previously in single-wave runup. One possible explanation is that most experimental

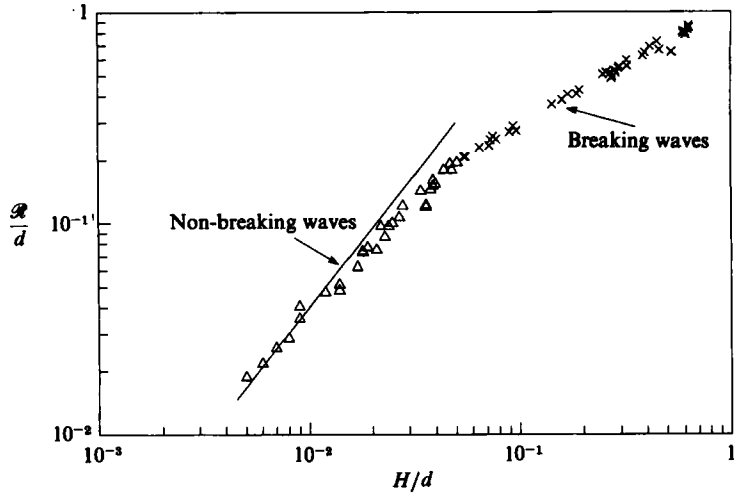

FIGURE 3. The normalized maximum runup of solitary waves up a 1:19.85 beach versus the normalized wave height. The data shown are listed in table 1. ×, breaking waves; △, non-breaking waves; ——, the runup law, (3.7).

investigations have dealt primarily with breaking solitary waves, and, even when non-breaking-wave data were generated, they were grouped together with breaking-wave data for the purpose of deriving empirical relationships.

To verify this observation and to draw conclusions about the application of the asymptotic result to other beaches, table 2 compares the runup law to published numerical results on non-breaking solitary-wave runup. The table illustrates that the asymptotic result agrees with the numerical results satisfactorily, except in the 45° case. However, the asymptotic result was derived assuming that $(H/d)^{\frac{1}{4}} \gg 0.288 \tan\beta$, and it is not expected to be formally correct when $\tan\beta = 1$. In this case, maximum-runup results derived from (3.4) agree with the numerical data much better.

Comparisons of analytical results with the Hall & Watts (1953) laboratory data are not as straightforward as often assumed. That study includes both breaking- and non-breaking-wave data without differentiating between them; empirical runup relationships derived there are not directly applicable when determining the runup of non-breaking waves. To perform *a posteriori* identification of those data, the breaking criterion $H/d < 0.479(\cot\beta)^{\frac{10}{9}}$ was used; it has been reported to be in excellent agreement with laboratory data for solitary waves (Gjevik & Pedersen 1981) and it is discussed in §6. Figure 4 presents all the non-breaking solitary-wave data from that and from other studies. The asymptotic result does seem to model the existing laboratory data satisfactorily. Note that non-breaking data are not yet available for $\cot\beta > 20$, and with good reason. On a 1:100 slope, the highest non-breaking wave is the wave with $H/d \approx 0.003$; such small waves are difficult to measure and they need a long propagation distance to develop fully.

The identification of the non-breaking-wave data in the Hall & Watts data set and its comparison with the runup law (3.7) offer some insight for the reasons why the two regimes in solitary-wave runup have been previously overlooked in the numerical work. Kim *et al.* (1983) studied the runup of non-breaking waves on steep beaches; their comparison with the Hall & Watts data revealed no significant discrepancies because most of the Hall & Watts data for steep slopes refer to non-

Depth (cm)	H/d	$\mathscr{R}/d$	Depth (cm)	H/d	$\mathscr{R}/d$
6.25	0.250	0.506	26.38	0.267	0.507
6.25	0.072	0.233	28.43	0.039	0.152
8.01	0.448	0.723	28.55	0.040	0.156
9.79	0.078	0.251	29.14	0.021	0.076
9.79	0.384	0.621	29.34	0.014	0.049
9.81	0.097	0.274	29.35	0.051	0.191
9.84	0.462	0.659	29.40	0.075	0.258
9.89	0.236	0.467	29.54	0.073	0.248
13.17	0.294	0.542	29.62	0.065	0.228
14.54	0.610	0.780	29.63	0.055	0.207
14.54	0.591	0.790	29.72	0.056	0.207
14.54	0.607	0.805	29.73	0.034	0.144
14.54	0.607	0.780	29.75	0.018	0.074
15.50	0.601	0.801	29.77	0.009	0.036
15.67	0.090	0.270	29.80	0.018	0.075
15.72	0.259	0.519	29.83	0.027	0.108
15.76	0.590	0.810	29.86	0.038	0.146
15.62	0.298	0.551	30.00	0.047	0.195
15.65	0.322	0.591	30.48	0.047	0.195
15.69	0.170	0.407	30.93	0.188	0.425
16.70	0.273	0.487	30.97	0.019	0.078
17.53	0.276	0.495	31.06	0.019	0.076
19.42	0.633	0.842	31.38	0.094	0.288
19.42	0.625	0.825	33.31	0.009	0.041
19.47	0.626	0.862	33.52	0.005	0.019
19.56	0.283	0.527	33.55	0.006	0.022
19.62	0.286	0.513	33.61	0.007	0.026
20.80	0.323	0.555	33.65	0.028	0.123
20.85	0.036	0.124	33.65	0.008	0.029
20.92	0.188	0.409	33.76	0.023	0.087
20.92	0.271	0.513	33.84	0.017	0.063
20.92	0.416	0.686	34.04	0.024	0.098
21.01	0.159	0.384	34.24	0.012	0.048
21.44	0.160	0.384	34.29	0.014	0.052
21.47	0.143	0.366	34.39	0.009	0.036
22.08	0.036	0.121	35.35	0.193	0.426
23.49	0.394	0.641	37.97	0.044	0.182
24.00	0.048	0.182	37.99	0.022	0.098
			38.32	0.039	0.162

TABLE 1. The runup of solitary waves up a 1:19.85 beach. Laboratory data.

breaking waves. In the study of Pedersen & Gjevik (1983), the discrepancy of the numerical results for mild slopes with extrapolated values from the Hall & Watts study is obvious; for mild-slope beaches most of the Hall & Watts data refer to breaking waves. Pedersen & Gjevik reference other solitary-wave experiments and note that their numerical results agree with laboratory data in water of 25 cm depth much better than they do in water of 10 cm depth. Although it has not been possible to obtain the reference data set, it can be hypothesized that the 25 cm depth data set included more non-breaking-wave data than the 10 cm depth set; it is easier to generate non-breaking waves in deeper water.

Source	$\cot\beta$	H/d	$\mathscr{R}/d$ Numerical calculations	$\mathscr{R}/d$ Runup law $2.831X_0^{\frac{1}{4}}(H/d)^{\frac{1}{2}}$	$\mathscr{R}/d$ Laboratory experiments
H&H	10.000	0.030	0.100	0.112	na
H&H	10.000	0.050	0.180	0.212	na
KLL	3.732	0.050	0.135	0.129	0.173
KLL	3.732	0.100	0.308	0.308	0.281
KLL	3.732	0.200	0.766	0.732	0.599
H&H	3.333	0.050	0.150	0.122	na
H&H	3.333	0.100	0.310	0.291	na
P&G	2.747	0.050	0.127	0.111	0.115
P&G	2.747	0.098	0.275	0.257	0.252
P&G	2.747	0.193	0.599	0.600	0.552
P&G	2.747	0.294	0.958	1.016	0.898
KLL	1.000	0.060	0.129	0.084	0.115
KLL	1.000	0.100	0.159	0.159	0.212
KLL	1.000	0.200	0.504	0.379	0.454
KLL	1.000	0.480	1.610	1.131	1.270

TABLE 2. Runup data from numerical calculations. H&H: Heitner & Housner (1970); KLL: Kim *et al.* (1983); P&G: Pedersen & Gjevik (1983). The runup-law column lists results derived by using (3.7). The laboratory-experiments column shows results derived from interpolation of the Hall & Watts (1953) data set, when possible.

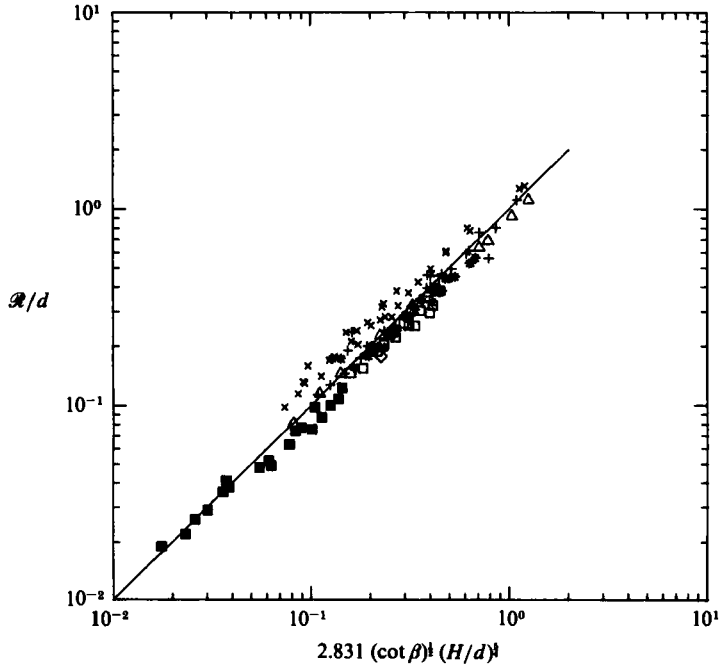

FIGURE 4. The normalized maximum runup of solitary waves climbing up different beaches versus the normalized wave height. ■, $\cot\beta = 19.85$, Synolakis (1986); ◇, $\cot\beta = 11.43$, Hall & Watts (1953); □, $\cot\beta = 5.67$, Hall & Watts (1953); *, $\cot\beta = 3.373$, Hall & Watts (1953); △, $\cot\beta = 2.75$, Pedersen & Gjevik (1983); +, $\cot\beta = 2.14$, Hall & Watts (1953); ×, $\cot\beta = 1.00$, Hall & Watts (1953); ——, the runup law, (3.7).

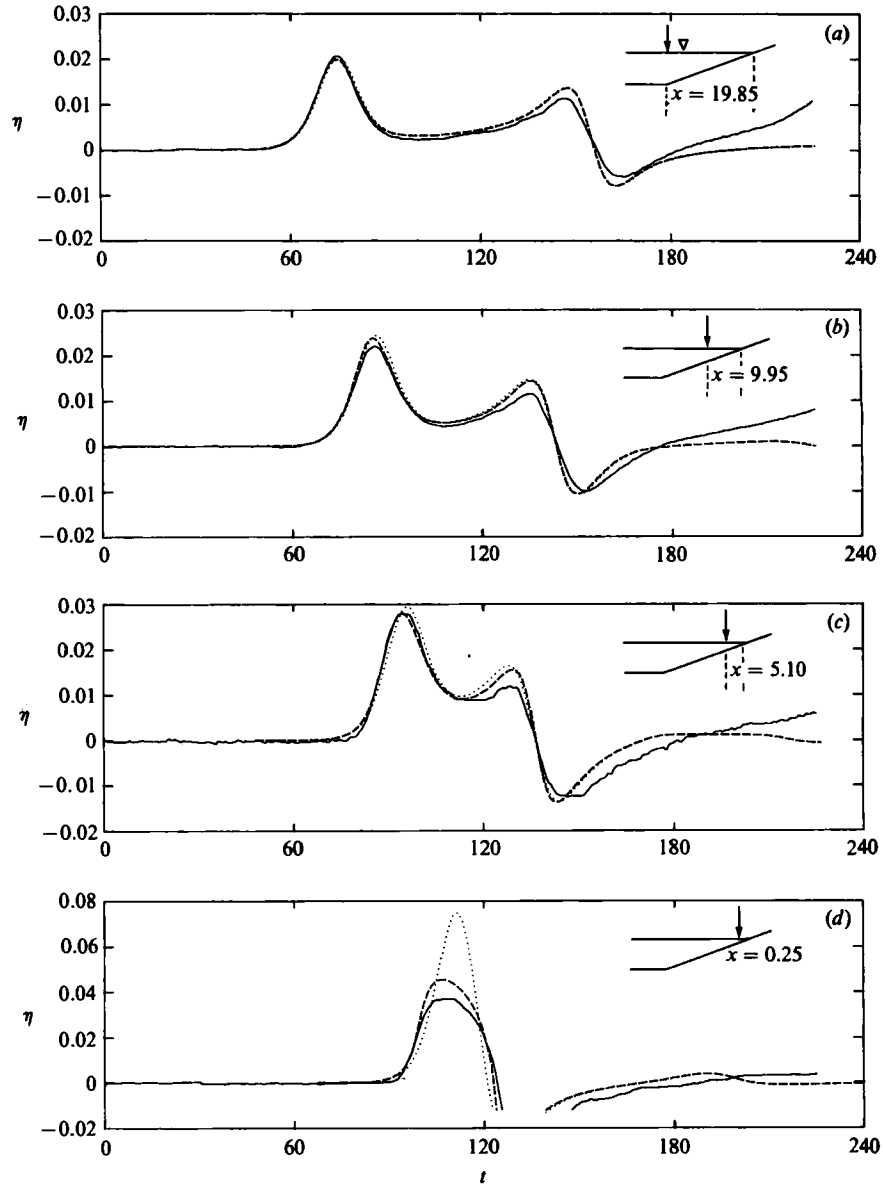

FIGURE 5. The climb of a solitary wave with $H/d = 0.019$ up a 1:19.85 beach. The normalized surface profiles are shown as functions of the normalized time at (*a*) $x = 19.85$, (*b*) 9.95, (*c*) 5.10 and (*d*) 0.25; ——, laboratory realization; – – –, nonlinear theory; · · · ·, linear theory.

5.2. *Amplitude evolution*

This section examines surface profiles in detail. Two different representations of the data are given: profiles showing the variation with time at fixed locations and profiles showing the variations in space at fixed times.

To derive surface profiles from the linear-theory solution, (3.2) can be substituted directly into (2.6), and then the integral can be evaluated with standard methods or with the solution method presented in the Appendix. Surface profiles for given (σ, λ) can be derived from the nonlinear theory explicitly using (3.8). However, to compare the theory with laboratory data it is necessary to obtain values at specific

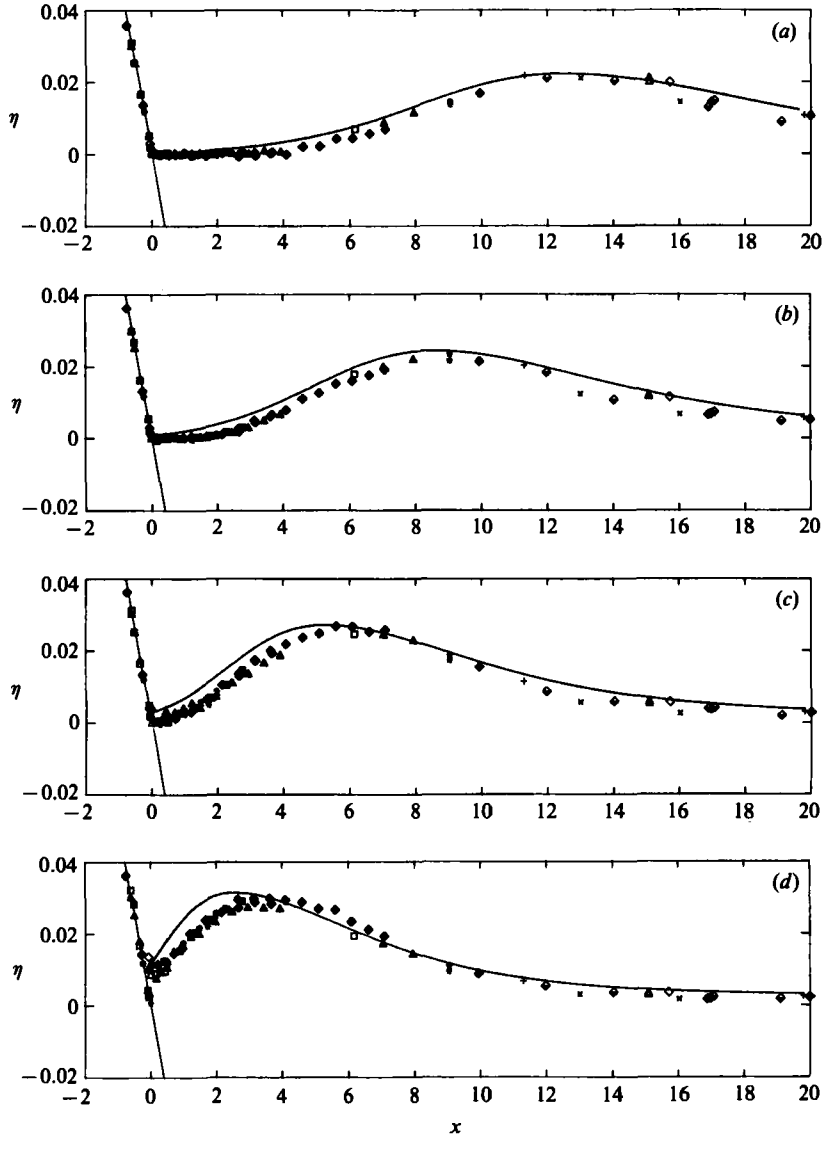

FIGURE 6(*a–d*). For caption see page 539.

points in the (x,t)-plane, i.e. at points where measurements exist. Since the transformation equations define η implicitly in terms of x and t, whenever the solution was required at a particular x or a particular t, (3.8*c*) and (3.8*d*) respectively were solved with the method of Newton's iterations. The iterations converged rapidly and with little computational effort.

Figure 5 shows the comparison among the linear-theory solution (2.6), the nonlinear-theory solution (3.8*b*), and the laboratory data for a solitary wave with $H/d = 0.019$ at four x-locations as a function of time. For $x = 19.85$, 9.95 and 5.10, there is no significant difference between the three profiles. However, closer to the shoreline nonlinear effects become important. Figure 5(*d*) shows the same incoming wave measured at a distance of 0.25 depths from the shoreline. The linear theory overestimates the wave height substantially. An interesting feature of this surface

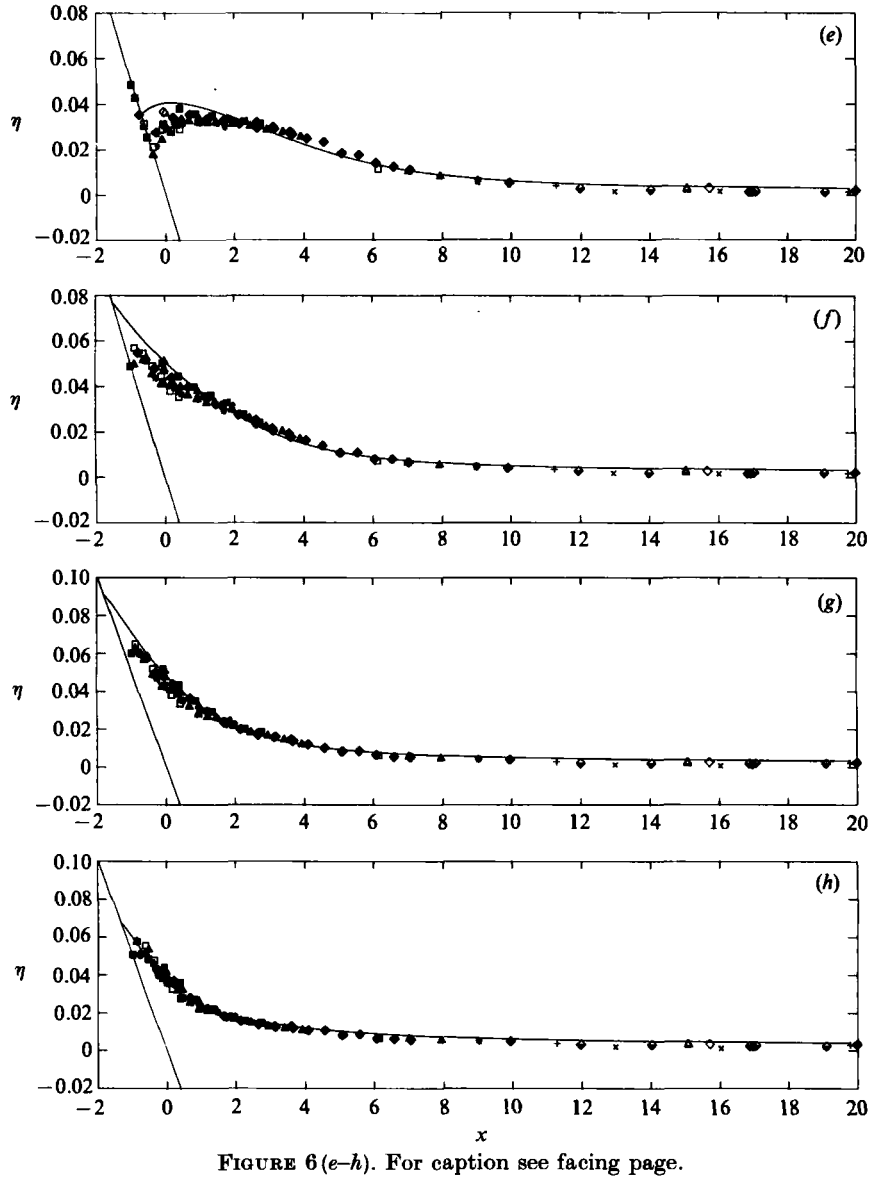

FIGURE 6 (e–h). For caption see facing page.

profile is its behaviour during the time interval from approximately $t = 125$ to 138, where there are no data displayed. This occurs during the backwash, when the shoreline retreats beyond that x-location, and there is no flow depth to be measured. The shoreline returns, but it does not stop moving at its initial position. The process of secondary runup begins and the shoreline behaves as an underdamped oscillator. This is a characteristic feature of the runup process and was observed in all the waves studied.

Figure 5 also helps explain Carrier's hypothesis. Carrier (1966) hypothesized that far from the shoreline nonlinear effects are small, so that the linear form of the transformation equations (2.10) can be used. It is seen that this is indeed an excellent approximation. The same conclusion can also be deduced from figure 4, where the theory is found to predict reasonable values even for waves with $H/d = 0.5$ climbing

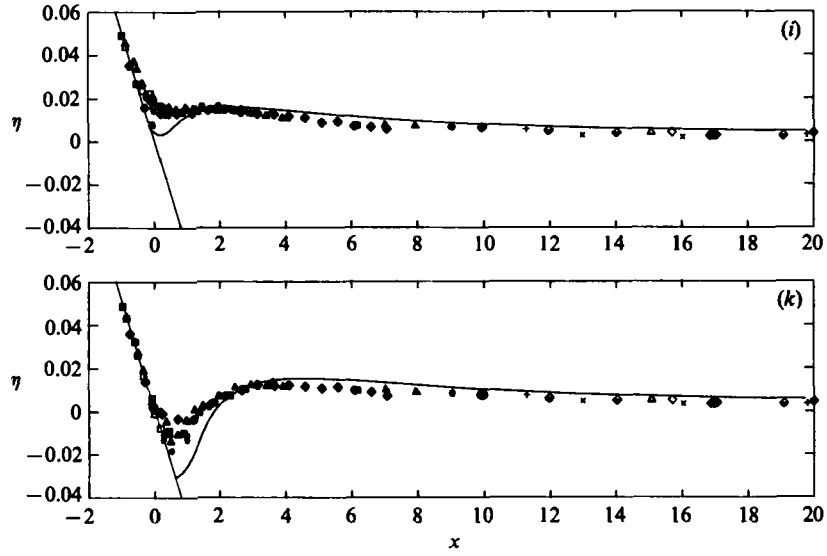

FIGURE 6. The climb of a solitary wave with $H/d = 0.019$ up a 1:19.85 beach. The normalized surface profiles are shown as functions of the normalized distance at different times, (*a*) $t = 25$, (*b*) 30, (*c*) 35, (*d*) 40, (*e*) 45, (*f*) 50, (*g*) 55, (*h*) 60, (*i*) 65, (*k*) 70; ——, nonlinear theory. The symbols indicate different realizations of the same initial conditions in the laboratory. All active measurement locations are shown, regardless of whether the wave has reached that location or not.

up a 45° slope, a case where the shoreline is only one depth away from the toe of the beach.

Figure 6 shows the amplitude evolution of a wave with $H/d = 0.019$ at different time instances as it climbs up the beach. The profiles presented can be visualized as still photographs of the surface. The nonlinear theory appears to predict the details of the climb of the wave on the beach adequately. Near the shoreline tip the theory overestimates the wave height, but this is to be expected as viscous effects are most significant in that region of the flow. The same behaviour can also be observed for the wave with $H/d = 0.04$, which is described in the next section.

6. Validity of the solution

The solution described in §2 is valid for functions $\Phi(k)$ such that the Jacobian of the transformation (2.7) is never equal to zero. The Jacobian becomes zero when the surface slope $\partial\eta/\partial x$ becomes infinite. In the physical plane this point is usually interpreted as the point of wave breaking. In this section a relationship will be derived between the limiting H/d of solitary waves climbing up a plane beach of slope β.

The Jacobian of the Carrier & Greenspan transformation is $\mathscr{J}$, and $\mathscr{J} = c(t_\sigma^2 - t_\lambda^2)$. Since it is anticipated that the transformation becomes singular close to the shoreline, the Jacobian is expanded around $\sigma = 0$. Substituting (2.7*c*) in the expression for the Jacobian and taking the limit as $\sigma \to 0$, then $\mathscr{J} \to (\frac{1}{4}\cot^2\beta)(u_\lambda - \frac{1}{2})^2$. Evaluating u with (3.8*a*), it follows that the Jacobian is always regular when

$$u_\lambda - \tfrac{1}{2} = -\tfrac{2}{3}X_0^2 \int_{-\infty}^{\infty} \frac{\kappa^3 \operatorname{cosech}(\alpha\kappa) \exp[\mathrm{i}\kappa(X_1 - X_0 + \frac{1}{2}\lambda X_0)]}{J_0(2\kappa X_0) - \mathrm{i}J_1(2\kappa X_0)} \mathrm{d}\kappa - \tfrac{1}{2} \neq 0. \qquad (6.1)$$

The integral can be evaluated with the formalism described in the Appendix, if one replaces the function z cosech αz in (A 2) with z^3 cosech αz. It can be verified by inspection that the radius of convergence of the resulting contour integral is the same as that of (A 1). The poles of the integrand are z_n, where $z_n = n\pi i/a$, and the residues are given by $-(n\pi/\alpha)^2 a_n$, where a_n is defined by (A 4). For large values of $4X_0\gamma$, the terms of the resulting Laurent series can be replaced by their asymptotic form. Then,

$$u_\lambda = -12(\pi\sqrt{3})^{\frac{1}{2}} X^{\frac{5}{2}} \left(\frac{H}{d}\right)^{\frac{9}{4}} \sum_{n=1}^{\infty} (-1)^{n+1} n^{\frac{7}{2}} \exp\left[-(3H/d)^{\frac{1}{2}}(X_1 + X_0 + \tfrac{1}{2}\lambda X_0)\right]. \quad (6.2)$$

The series $\Sigma_{n=1}^{\infty}(-1)^n n^{\frac{7}{2}} x^n$ attains its minimum value of -0.02847 when $\chi = 0.06530$. This value defines the limiting H/d when $u_\lambda - \frac{1}{2}$ goes through zero, as

$$\frac{H}{d} = 0.8183(\cot\beta)^{-\frac{10}{9}}. \quad (6.3)$$

This is a weaker restriction than that derived by Gjevik & Pedersen (1981), who determined that waves break when

$$\frac{H}{d} > 0.479(\cot\beta)^{-\frac{10}{9}}. \quad (6.4)$$

However, there are two basic differences between the two results. The Gjevik & Pedersen criterion (6.4) indicates the limiting H/d when a solitary wave breaks during the backwash. Equation (6.3) indicates when a wave first breaks during runup. It is therefore not surprising that the former is a stronger criterion; long waves that do not break during runup may break during rundown. Also, the Gjevik & Pedersen result (6.4) was derived by using the sinusoidal wave profile that best fits the Boussinesq profile. Equation (6.3) is based on the actual Boussinesq profile (3.1).

The breaking criteria (6.3) and (6.4) imply that as $\cot\beta \to \infty$ then the limiting $H/d \to 0$, while on steep beaches, as $\cot\beta \to 0$, the theory is valid for relatively large H/d. This is entirely consistent with the non-dispersive nature of the theory. On very gentle beaches where the propagation distances are large the theory applies for very small waves only; on steep beaches the propagation distances are small, and dispersive effects do not have sufficient time to develop fully.

To visualise the two different breaking criteria, it is helpful to examine the Jacobian of the Carrier & Greenspan transformation in detail. Figure 7 shows $u_\lambda - \frac{1}{2}$ as a function of λ as $\sigma \to 0$, for the particular case when $H/d = 0.040$ and $X_0 = 19.85$. As λ decreases, the Jacobian first becomes zero at $\lambda = \lambda_{c_0}$. The first local maximum of u_λ occurs at $\lambda = \lambda_{c_1}$. This local maximum was used to determine the limiting H/d in (6.3) through the series (6.2). The global maximum of u_λ occurs at $\lambda = \lambda_{c_2}$. This maximum corresponds to the criterion (6.4). It is the particular property of this Jacobian, that $\mathrm{Re}\, u_\lambda(0, \lambda_{c_2}) > \mathrm{Re}\, u_\lambda(0, \lambda_{c_1})$ and $\lambda_{c_1} > \lambda_{c_2}$, that predetermines that wave breaking will first occur during the rundown.

It is a well-documented phenomenon that the shallow-water-wave formalism usually predicts wave breaking earlier than it actually happens in nature. It is interesting to examine what the theory predicts for the climb of solitary waves that are larger than the limiting value implied by both (6.3) and (6.4), but that do not break when realized in the laboratory. For the laboratory beach, (6.4) predicts that breaking first occurs in the backwash when $H/d > 0.017$, while (6.3) implies that waves break during runup when $H/d > 0.029$. Consider the climb of a wave with $H/d = 0.040$. (This is the wave whose Jacobian is shown in figure 7.) Figure 8 shows

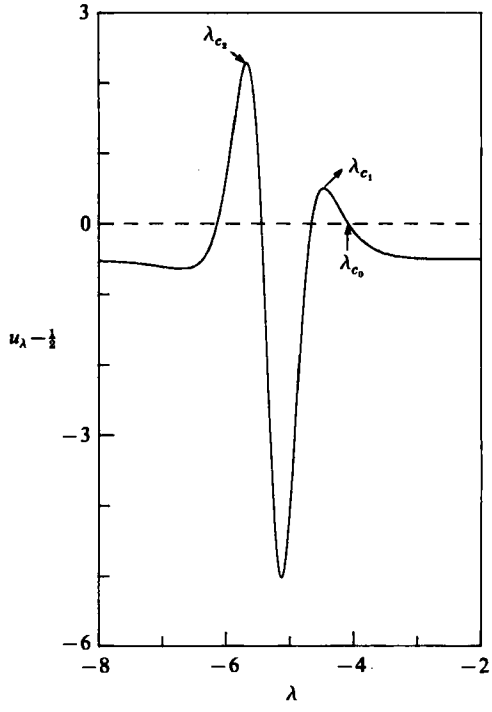

FIGURE 7. The Jacobian of the Carrier & Greenspan transformation when $H/d = 0.040$ and $\cot\beta = 19.85$, expanded around $\sigma = 0$.

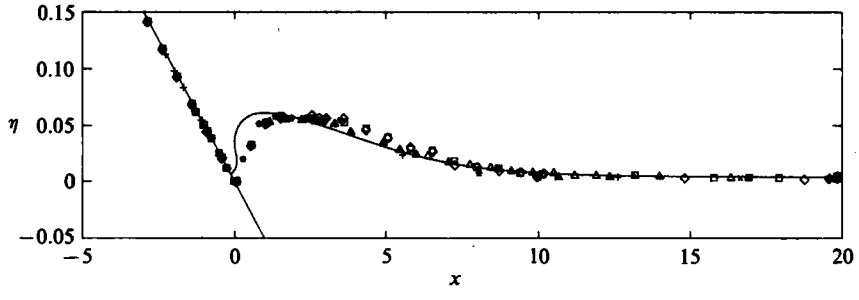

FIGURE 8. The normalized surface profile of a solitary wave with $H/d = 0.040$ up the laboratory beach, approximately when the Jacobian becomes singular, $t = 36$; ——, nonlinear theory.

the wave profile, approximately when the Jacobian first goes through zero. The solution becomes multivalued and the wave is seen to curl over. However, the laboratory realization of the same wave does not exhibit breaking.

On intuitive grounds it is expected that beyond λ_{c_0} (where $\partial\eta/\partial x \to \infty$) any transformation of results back to the (x, t)-plane will be meaningless. This is also suggested from the existing numerical simulations of the climb of breaking waves, where the solution becomes unbounded soon after the slope of the wavefront becomes infinite. It is therefore surprising to discover that the analytical solution recovers and subsequent surface profiles are stable, well-defined, continuous functions. The same behaviour was observed by Tuck & Hwang (1972) when they attempted to calculate surface profiles beyond breaking. They noted that the linear-theory solution could be formally recovered from the post-breaking profiles, and they speculated that they

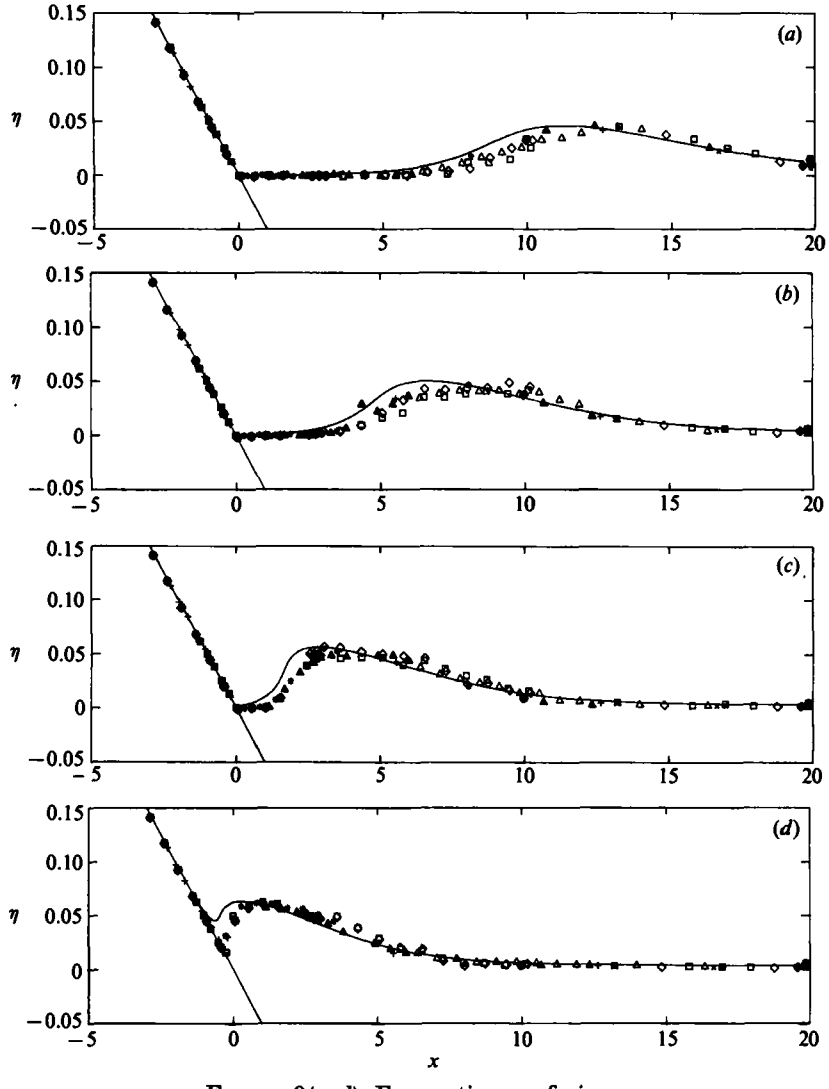

FIGURE 9(*a–d*). For caption see facing page.

should have practical significance. It is intriguing to observe how well these profiles compare with those realized in the physical model. Figure 9(*a*, *b*, *c*) shows surface profiles before, and figure 9(*d*, *e*, *f*, *g*, *h*) shows profiles after, breaking. The nonlinear theory models the laboratory data equally well before and after breaking. The same phenomenon occurs during the rundown.

To understand this apparent paradox, one must realize that the solution beyond λ_{c_0} may not be the valid solution to the original boundary-value problem, but it is a valid solution to a new boundary-value problem with boundary values specified at $(0, \lambda_{c_0} + \delta\lambda)$. What figure 9 indicates is that the solution beyond breaking is relatively insensitive to the amplitude profile at breaking. This phenomenon appears to be a manifestation of the same process that allows for Whitham's bore rule which postulates that the solution for the problem of the climb of a bore up a beach may be determined, approximately, by applying the relationships valid at the bore front behind it, i.e. the details of the solution at the front may not be essential in the subsequent evolution of the wave.

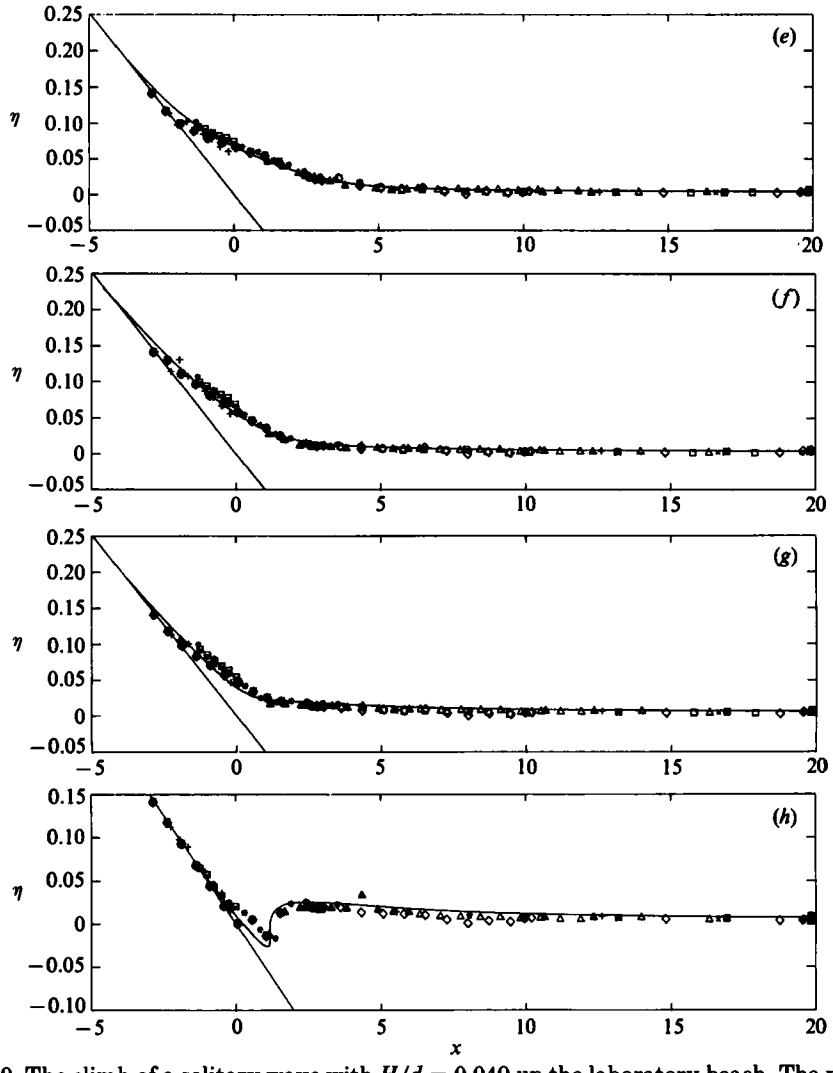

FIGURE 9. The climb of a solitary wave with $H/d = 0.040$ up the laboratory beach. The normalized amplitude surface profiles are shown as functions of the normalized distance at different times, (*a*) $t = 20$, (*b*) 26, (*c*) 32, (*d*) 38, (*e*) 44, (*f*) $t = 50$, (*g*) 56, (*h*) 62; ——, nonlinear theory. Breaking in the theoretical development occurs during runup at $t \approx 36$ and during the rundown at $t \approx 60$.

7. Summary and conclusions

In the previous sections a theory has been presented and an asymptotic result has been derived for the runup of non-breaking solitary waves on plane beaches. Detailed measurements of the runup height and of the climb of solitary waves have also been presented. There are four major conclusions:

(i) The linear and nonlinear theories predict that the maximum runup of non-breaking waves is given by the runup law (3.7):

$$\frac{\mathscr{R}}{d} = 2.831(\cot\beta)^{\frac{1}{2}}\left(\frac{H}{d}\right)^{\frac{5}{4}}.$$

(ii) The runup variation is different for breaking and non-breaking solitary waves.

(iii) Surface profiles derived from the nonlinear theory model the climb of non-breaking waves adequately.

(iv) Different criteria apply for determining if a solitary wave of given height-to-depth ratio will break as it climbs up a sloping beach and for determining if it will break during the rundown.

I would like to thank Fred Raichlen for suggesting the topic and for arranging for the funding of the laboratory study through grants from the National Science Foundation and the California Institute of Technology. Funding was also provided by the Alexander Onassis Public Benefit Foundation and the University of Southern California. I am grateful to George Carrier, Bob Guza and Fred Browand for many interesting suggestions.

Appendix. Evaluation of the runup integral

Consider the integral $I_{\mathscr{C}}$ defined in the domain $\mathscr{D}$ in the upper half-plane bounded by the contour $\mathscr{C}$:

$$I_C(t) = \oint \frac{z \operatorname{cosech}(\alpha z)\, e^{iz\theta}}{J_0(2X_0 z) - iJ_1(2X_0 z)} dz,$$

where $\theta = X_1 - X_0 - ct$. The contour $\mathscr{C}$ consists of a positively oriented semicircle of radius $|z| = r$, $0 < \arg z < \pi$ with its centre at the origin and of the real-axis segment $(-r, r)$. The integral converges in $\mathscr{D}$ for all θ such that $-(2X_0 + \theta)|\operatorname{Im} z| < \alpha |\operatorname{Re} z|$. For arbitrary α, the integral converges $\forall t$ such that

$$X_1 + X_0 - ct > 0.$$

When $\operatorname{Im} z < 0$, the integral converges in the sector defined by

$$\alpha|\operatorname{Re} z| + (X_1 - 3X_0 - ct)|\operatorname{Im} z| < 0.$$

The function $J_0(z) - iJ_1(z)$ has no zeroes in the upper half-plane (Synolakis 1988). The only poles of the integrand inside $\mathscr{D}$ are then the poles of numerator, $z_n = n\pi i/\alpha, n = 1, 2, 3 \ldots$. The residue at these poles is a_n, given by

$$a_n = \frac{(-1)^n \left(\frac{n\pi}{\alpha^2}\right) \exp\left(-\frac{n\pi}{\alpha}\theta\right)}{J_0\left(2X_0 \frac{n\pi}{\alpha} i\right) - iJ_1\left(2X_0 \frac{n\pi}{\alpha} i\right)} i.$$

Then, by the Cauchy integral formula

$$I_{\mathscr{C}}(t) = \frac{2\pi^2}{\alpha^2} \sum_{n=1}^{\infty} \frac{(-1)^{n+1} n\, e^{-2\gamma\theta n}}{I_0(4\gamma X_0 n) + I_1(4\gamma X_0 n)}.$$

$I_{\mathscr{C}}(t)$ can be broken into two integrals: one integral $I_r(t)$ along the real axis and another $I_0(t)$ along the semicircle. For large r, $I_\theta(t) \to 0$ by Jordan's lemma. Then $I_{\mathscr{C}}(t) = I_r(t)$ and (3.4) follows directly.

REFERENCES

Battjes, J. A. & Roos, A. 1971 Characteristics of flow in the run-up of periodic waves. *Rep.* 75–3. Dept. of Civil Engineering, Delft University of Technology. 160 pp.

Camfield, F. E. & Street, R. L. 1969 Shoaling of solitary waves on small slopes. *Proc. ASCE* **WW95**, 1–22.

CARRIER, G. F. 1966 Gravity waves of water of variable depth. *J. Fluid Mech.* **24**, 641–659.

CARRIER, G. F. 1971 The dynamics of tsunamis. In *Mathematical Problems in the Geophysical Sciences. Proc. 6th Summer Seminar on Applied Mathematics, Rennselar Polytechnic Institute, Troy, NY, 1970.* American Mathematical Society.

CARRIER, G. F. & GREENSPAN, H. P. 1958 Water waves of finite amplitude on a sloping beach. *J. Fluid Mech.* **17**, 97–110.

CARRIER, G. F., KROOK, M. & PEARSON, C. E. 1966 *Functions of a Complex Variable.* McGraw Hill. 438 pp.

GJEVIK, B. & PEDERSEN, G. 1981 *Run-up of long waves on an inclined plane. Preprint Series Inst. of Math. Univ. of Oslo,* ISBN 82-553-0453-3.

GORING, D. G. 1978 Tsunamis – the propagation of long waves onto a shelf. *Rep.* KH-R-38. W. M. Keck Laboratory of Hydraulics and Water Resources, California Institute of Technology, Pasadena, CA. 337 pp.

GUZA, R. T. & THORNTON, E. B. 1982 Swash oscillations on a natural beach. *J. Geophys. Res.* **87**, 483-491.

HALL, J. V. & WATTS, J. W. 1953 Laboratory investigation of the vertical rise of solitary waves on impermeable slopes. *Tech. Memo.* 33, Beach Erosion Board, US Army Corps of Engineers. 14 pp.

HAMMACK, J. L. 1972 Tsunamis – A model of their generation and propagation. *Rep.* KH-R-28. W. M. Keck Laboratory of Hydraulics and Water Resources, California Institute of Technology, Pasadena, CA. 261 pp.

HEITNER, K. L. & HOUSNER, G. W. 1970 Numerical model for tsunami run-up. *Proc. ASCE* **WW3**, 701–719.

HIBBARD, S. & PEREGRINE, D. H. 1979 Surf and run-up on a beach : a uniform bore. *J. Fluid Mech.* **95**, 323–345.

HOLMAN, R. A. 1986 Extreme value statistics for wave runup on a natural beach. *Coastal Engng* **9**, 527–544.

KELLER, J. B. & KELLER, H. B. 1964 *Water wave run-up on a beach. ONR Research Rep. Contract* NONR-3828(00). Dept. of the Navy, Washington, D.C. 40 pp.

KIM, S. K., LIU, P. L-F. & LIGGETT, J. A. 1983 Boundary integral equation solutions for solitary wave generation propagation and run-up. *Coastal Engng* **7**, 299–317.

KISHI, T. & SAEKI, H. 1966 The shoaling, breaking and runup of the solitary wave on impermeable rough slopes. In *Proc. ASCE, Tenth Conference on Coastal Engineering, Tokyo, Japan,* pp. 322–348.

LEWY, H. 1946 Water waves on sloping beaches. *Bull. Am. Math. Soc.* **52**, 737–755.

MEYER, R. E. 1986 On the shore singularity of water wave theory. II. Small waves do not break on gentle beaches. *Phys. Fluids* **29**, 3164–3171.

PEDERSEN, G. & GJEVIK, B. 1983 Run-up of solitary waves. *J. Fluid Mech.* **135**, 283–290.

SPIELVOGEL, L. Q. 1974 Single-wave runup on sloping beaches. *J. Fluid Mech.* **74**, 685–694.

STOKER, J. J. 1947 Surface waves in water of variable depth. *Q. Appl. Maths* **5**, 1–54.

SYNOLAKIS, C. E. 1986 The runup of long waves, Ph.D. thesis, California Institute of Technology, Pasadena, California, 91125. 228 pp.

SYNOLAKIS, C. E. 1988 On the zeros of $J_0(z) - iJ_1(z)$. *Q. Appl. Maths* (In press).

TUCK, E. O. & HWANG, L. 1972 Long wave generation on a sloping beach, *J. Fluid Mech.* **51**, 449–461.

ZELT, Z. A. 1986 Tsunamis: The response of harbors with sloping boundaries to long wave excitation. *Rep.* KH-R-47. W. M. Keck Laboratory of Hydraulics and Water Resources, California Institute of Technology, Pasadena, CA. 318 pp.